ISSN 1990-3413, Astrophysical Bulletin, 2013, Vol. 68, No. 2, pp. 169–176. © Pleiades Publishing, Ltd., 2013.
Original Russian Text © S.A. Alexeeva, A.M. Sobolev, S.Yu. Gorda, M.V. Yushkin, V. McSwain, 2013, published in Astrofizicheskij Byulleten, 2013, Vol. 68, No. 2, pp. 178–186.

Orbital and Physical Parameters of the Spectroscopic Binary HD 37737

S. A. Alexeeva[1], A. M. Sobolev[2], S. Yu. Gorda[2], M. V. Yushkin[3], and V. McSwain[4]

[1] *Institute of Astronomy of the RAS, Moscow, 119017 Russia*
[2] *Kourovka Astronomical Observatory, Ural Federal University, Ekaterinburg, 620000 Russia*
[3] *Special Astrophysical Observatory, Russian Academy of Sciences, Nizhnii Arkhyz, 369167 Russia*
[4] *Lehigh University, Bethlehem, PA 18015 USA*

Received October 29, 2012; in final form, February 28, 2013

Abstract—We report the physical and orbital parameters of the visible component of the spectroscopic binary HD 37737 ($m_V = 8.03$). The observations were performed with the 1.2-m telescope of the Kourovka Astronomical Observatory of the Ural Federal University in 2012 and the 6-m BTA telescope of the SAO RAS in 2007 and 2009. Radial velocities were measured separately from each spectral line of the list by the cross-correlation method with a synthetic spectrum. The latter was calculated using the grids of non-LTE model atmospheres with solar chemical compositions. A significant difference in the epochs of observations (2005–2012) allowed to refine the orbital period of the star ($7\overset{d}{.}84705$) and the orbital elements of the binary system. We obtained an estimate of the mass function $f(m) = 0.23 \pm 0.02\ M_\odot$. The best agreement between the synthetic and observed spectra is achieved at $T_{\rm eff} = 30\,000$ K and $\log g = 3.50$ according to the observations on both instruments. The obtained parameters correspond to a star of spectral type O9.5 III, with mass estimated at $26 \pm 2\ M_\odot$. The minimum mass estimate of the secondary component of the binary is $6.2 \pm 0.5\ M_\odot$. We have discovered a fact that the velocities, obtained from different spectral lines, differ, which is typical for giant stars. Engaging additional spectra, obtained in 2005 with the 2.1-m KPNO telescope, we investigated the effect of this fact on the estimate of the speed of the system's center of mass. The difference in the velocities of various lines is approximately the same in the spectra, obtained at all the three instruments. The obtained ratios suggest that the deeper layers of the atmosphere of the star are moving with a greater velocity than the outer layers. Depending on the line, the estimate of the heliocentric velocity of the binary's center of mass varies in the range from −11 to 1 km/s.

DOI: 10.1134/S1990341313020041

Keywords: *binaries: spectroscopic—stars: massive—stars: individual: HD 37737*

1. INTRODUCTION

The star HD 37737 is the central star of the nebula Sh2-232, located in the Perseus arm. Particular interest to this star is caused by the fact that owing to its high spatial velocity $V_{\rm pec} = 28.6 \pm 14.3$ km/s it is a runaway star candidate. Gies and Bolton found that this star is a spectroscopic binary and presented the first solution of its orbit [1]. They determined that the visible component of the system has an O9.5 III spectral type and $m_V = 8.03$. According to the results of subsequent observations, McSwain et al. [2] have refined the period of $7\overset{d}{.}84$, the value of the radial velocity half-amplitude, orbital elements and estimated the speed of the system's center of mass. The difference in the velocities, determined from various lines was noted. This is known for a number of stars. For example, in the atmosphere of supergiants, the difference in the velocities, determined from various lines can reach up to 140 km/s [3].

This work is based on the results of the new observations, performed at the new Kourovka Astronomical Observatory 1.2-m telescope of the Ural Federal University and the 6-m telescope of the Special Astrophysical Observatory of the Russian Academy of Sciences (SAO RAS). Our aim was to clarify the physical parameters and the parameters of the orbit of the HD 37737 spectroscopic binary system.

2. OBSERVATIONS

The present study has made use of the spectra obtained in 2005–2012 with the instruments of three observatories: Kourovka Astronomical Observatory, Special Astrophysical Observatory of the RAS, and Kitt Peak National Observatory (KPNO, USA). General characteristics of the spectra obtained with Russian instruments are presented in Table 1. The observations made at the KPNO are described in [2]. All the obtained spectra, just like the previously

Table 1. General description of the observations

№	JD 2454000+	Spectral range, Å	$n \times t_{\rm exp}$, min	R	$\langle S/N \rangle$
	BTA, 6-m				
1	375.374	5210–6690	1 × 60	60 000	200
2	1141.381	4000–5450	1 × 60	60 000	120
3	1141.422	4000–5450	1 × 60	60 000	120
4	1141.464	4000–5450	1 × 60	60 000	80
5	1141.506	4000–5450	1 × 60	60 000	80
6	1141.584	4000–5450	1 × 60	60 000	260
	KAO, 1.2-m				
7	1945.369	4000–7800	3 × 20	30 000	36
8	1946.411	4000–7800	3 × 20	30 000	36
9	1952.178	4000–7800	3 × 20	30 000	20
10	1952.448	4000–7800	3 × 20	30 000	20
11	1953.411	4000–7800	4 × 20	30 000	20
12	1953.451	4000–7800	3 × 20	30 000	25
13	1973.447	4000–7800	3 × 20	30 000	20
14	1978.384	4000–7800	3 × 20	30 000	36
15	1978.260	4000–7800	4 × 20	30 000	36

published data, reveal the lines of only one component of the spectroscopic binary.

2.1. Observations at KAO UFU 1.2-m Telescope

The observations of HD 37737 with the 1.2-m telescope ($D = 1.21$ m, $F = 12.0$ m) of the Kourovka Astronomical Observatory of the Ural Federal University [4] using a fiber optic echelle spectrograph [5] were conducted in January–February 2012. Nine echelle spectra with the spectral resolution of $R = 30\,000$ were obtained. The light detector used was a CCD camera, manufactured by the SAO RAS Advanced Design Laboratory, and equipped with a CCD chip E2V 40-42 (2048×2048 px, pixel size is 13.5μm), cooled to the temperature of around −130°C using the CRYOTIGER closed-loop system. The chip simultaneously recorded 60 spectral orders, covering the region of $\lambda\lambda$ 4000–7800 Å. In the process of acquisition of each CCD frame of the stellar spectrum, manual guiding was done via moving the telescope at low speed, controlled on screen by the image, given by the guide camera of the focal field of the telescope. The exposure of each frame was 20 minutes. At least three spectra of the star were obtained during one observational set. Immediately before and after imaging each triad, we recorded the spectra of the thorium-argon lamp. Subsequently, a series of three exposures was summarized, which allowed to remove the traces of cosmic ray particles and increase the signal-to-noise ratio (S/N). Thus, the effective exposure of each spectrum used in the further work amounted to 1 hour. The S/N ratio in the resulting spectra was at least 20, which, combined with the specified resolution, allowed to measure the position of lines, to describe the profile shapes, and calculate radial velocities by cross-correlation with a good accuracy.

The initial reduction of the CCD images, carried out in the context of the MIDAS `ECHELLE` package included:

1) averaging of the bias frames with their subsequent subtraction from the other frames, obtained during the observations;

2) subtraction of scattered light;

3) flat field reduction;

4) extraction of spectral orders;

5) construction of the dispersion curves for the spectra of a hollow cathode (ThAr) lamp for the conversion from counts to wavelengths.

The final reduction was performed in the specialized `DECHfits` code [6], which, in particular, can be used for:

1) continuum normalization;

2) spectrum smoothing by a median filter;

3) radial velocity measurements by the cross-correlation method.

The strongest lines in the spectra are the lines of helium He I and He II, as well as the lines of the Balmer series of hydrogen. With the achieved S/N ratio the remaining lines are not pronounced.

2.2. Observations at SAO RAS 6-m BTA Telescope

Observations at the 6-m BTA telescope of the SAO RAS with the NES spectrograph [7] were held in 2007 and 2009. In October 2007, we obtained one spectrum with a 1-h exposure in the region of $\lambda\lambda$ 5210–6690 Å, and five spectra were obtained in November 2009 with a 1-h exposure each in the region of $\lambda\lambda$ 4000–5450 Å. All the echelle spectra were obtained with the spectral resolution of $R = 60\,000$.

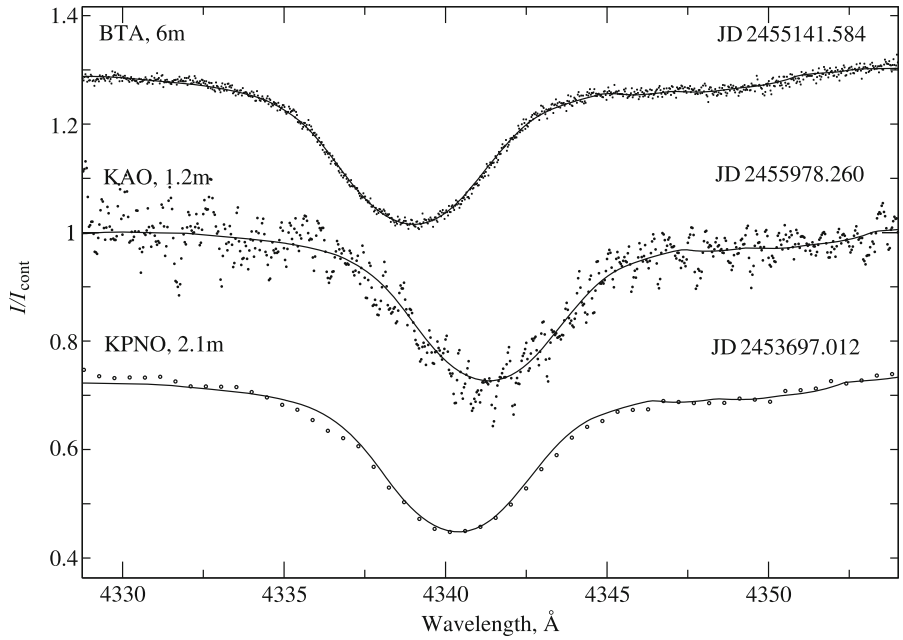

Fig. 1. Continuum-normalized Hγ line profiles according to the data of different instruments. The continuous line shows the theoretical spectrum. The lines are shifted relative to the mean profile at 0.28.

Initial reduction of the CCD images was conducted within the context of the MIDAS `ECHELLE` package.

The spectra obtained at the BTA have the S/N ratio of 260. The lines of the Balmer series of hydrogen, helium He I, II, and lines of heavy elements N II, III, O II, Si III, IV, C III, Ne II, Al III, Mg II, S III are confidently distinguished. In addition, the interstellar absorption lines of Ca I λ 4226.73 Å, CH+ λ 4232.54 Å, CH λ 4300.32 Å and Na I $\lambda\lambda$ 5889.95, 5895.92 Å are clearly visible.

2.3. Observational Data from KPNO 2.1-m Telescope

We used the files with 15 spectra of HD 37737 that were prepared and underwent initial reduction. They were obtained in October and November 2005 at the KPNO 2.1-m telescope in the range of $\lambda\lambda$ 4050–4950 Å with a high S/N ratio and the spectral resolution of $R = 3000$, reduced in the IRAF system. A more detailed description of the observations is given in [2]. A comparison of the Hγ line contours, obtained at different instruments is shown in Fig. 1.

3. ORBITAL SOLUTION

3.1. Radial Velocities

Radial velocities were determined in the `DECHfits` package by cross-correlation of the line profiles of the obtained spectra and a synthetic spectrum with the parameters and calculation method, described in Section 4.2. Tables 2 and 3 list the heliocentric radial velocities of different lines. The measurement errors of radial velocities were estimated by the formula:

$$\sigma_{V_r} = \frac{3\omega}{8(1+f)}, \qquad (1)$$

where ω is the FWHM of the correlation function, f is the ratio of the correlation peak height to the antisymmetric noise amplitude [8].

Since the velocities vary with phase due to the orbital motion of the star, for the further analysis the velocities of individual lines were reduced to relative values—residual velocities. To do this, we subtracted from the velocity measurements the mean velocity at the time of observation, averaged over the lines, listed in Tables 2 and 3.

The dependences of residual velocities on the residual intensity (r), equivalent width (EW) and excitation potential of the lower line level (IPl) (see Fig. 2). To estimate the correlation ratio between the values, we calculated the linear correlation coefficient for each set of dependences (see the bottom left corner of each panel in Fig. 2). In all cases, except for (i), the absolute value of the correlation coefficient is more than three times higher than its mean square error, confirming its importance. According to the data from all the instruments, the character of the dependence is the same: there is a general increase of residual velocity with increasing residual intensity

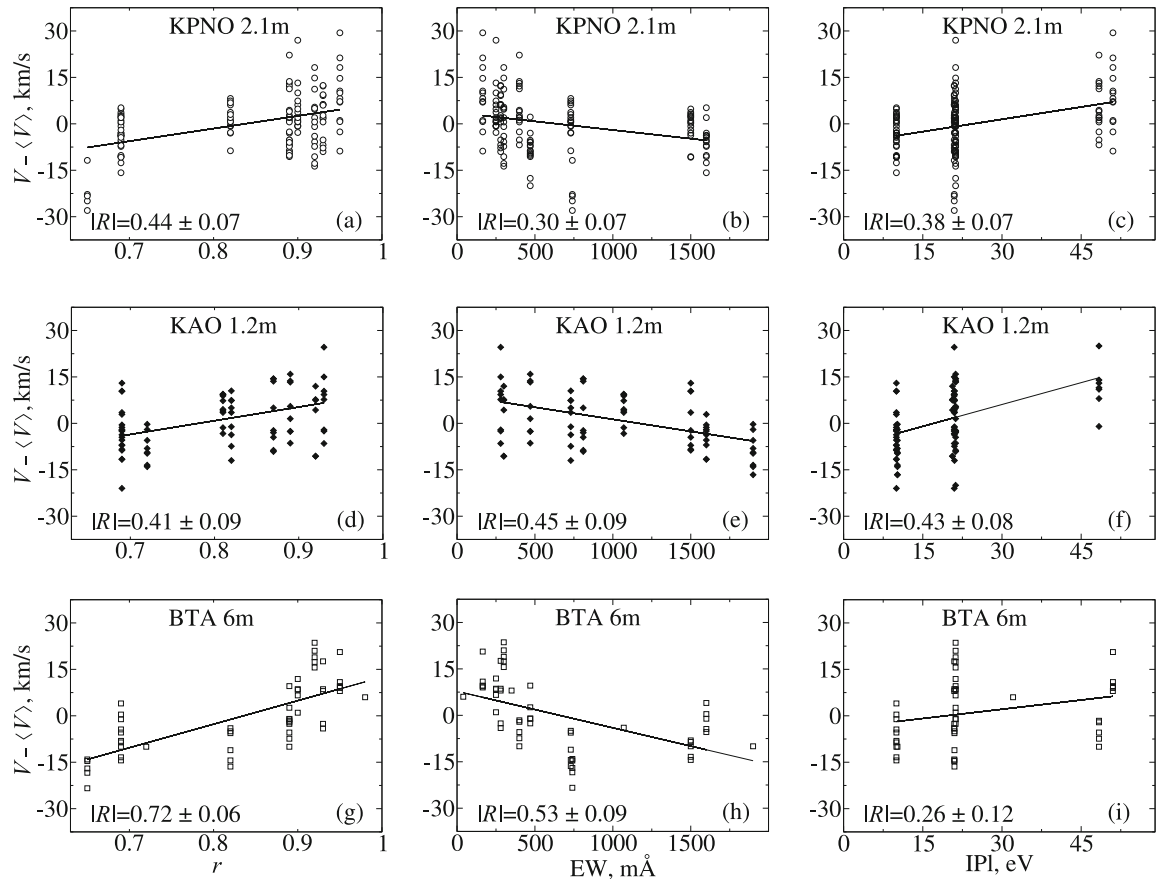

Fig. 2. Dependences of residual line velocity (the difference between the line velocity and the mean over the line set) on the residual intensity (left), equivalent width (center) and excitation potential (right) according to the data obtained at different instruments. Linear regressions demonstrate general trends. All the dependences differ from constant. This indicates the existence of a velocity gradient in the stellar atmosphere.

and excitation potential of the lower line level, and a velocity decrease with the growth of the equivalent line width. The regression lines shown in Fig. 2 have a significant slope, which indicates that the lines, formed in different layers of the atmosphere, reveal different Doppler shifts. Apparently, the stellar atmosphere has a velocity gradient, which is a recognized fact for giants. Residual intensity of the absorption line declines with increasing optical thickness, hence, the lines with large residual intensities are formed in the deeper layers of the atmosphere than the lines with small residual intensities. Consequently, the velocity increase with growing residual intensity means that the deeper layers of the stellar atmosphere are moving away from us at a greater velocity than its outer layers. An rise of residual velocity with increasing excitation potential and its decline with an increase of the equivalent width supports this hypothesis.

3.2. Radial Velocity Curve

It follows from the previously published studies that the orbit of HD 37737 has a significant eccentricity. In this case, the theoretical curve of radial velocities is described by the following equation:

$$V_r(\theta) = V_{\rm cm} + K_1(\cos(\theta + \omega) + e\cos\omega), \qquad (2)$$

where $V_{\rm cm}$ is the heliocentric radial velocity of the center of mass; θ is the true anomaly; ω is the longitude of periastron; e is the orbit eccentricity; K_1 is the half-amplitude of the radial velocity curve. Since in our case the orbit has a significant eccentricity, for a more precise calculation of the true anomaly, instead of the iterative solution of Kepler's equation, we used a decomposition of the true anomaly in powers of

Table 2. Radial velocities obtained from the results of observations at the 6-m BTA telescope. The columns of radial velocities are arranged in the order of spectra 1 to 6 from Table 1

Line	r	V_r, km/s					
		1	2	3	4	5	6
Hβ 4861 Å	0.69		-62 ± 2	-60 ± 3	-57 ± 3	-65 ± 2	-78 ± 2
Hγ 4341 Å	0.69		-69 ± 2	-69 ± 3	-71 ± 3	-74 ± 2	-87 ± 2
Hα 6563 Å	0.72	4 ± 2					
He I 5876 Å	0.81	10 ± 2					
He I 4471 Å	0.82		-72 ± 2	-66 ± 3	-66 ± 3	-77 ± 3	-87 ± 3
He II 4686 Å	0.89		-63 ± 2	-62 ± 2	-71 ± 2	-68 ± 1	-78 ± 2
He I 4922 Å	0.89		-62 ± 3	-63 ± 3	-62 ± 3	-58 ± 3	-63 ± 3
He I 4388 Å	0.90		-49 ± 3	-52 ± 3	-60 ± 3	-52 ± 2	-66 ± 2
He I 4143 Å	0.92		-42 ± 3	-43 ± 3	-40 ± 2	-45 ± 2	-49 ± 2
He I 4713 Å	0.93		-65 ± 3	-63 ± 3	-53 ± 3	-43 ± 3	-64 ± 3
He II 4541 Å	0.95		-50 ± 3	-51 ± 4	-52 ± 4	-40 ± 3	-63 ± 3
He II 5411 Å	0.95	22 ± 3					
C III 5695 Å	0.98	20 ± 4					
Mean	–	14 ± 3	-61 ± 3	-60 ± 3	-61 ± 3	-61 ± 3	-73 ± 3

Table 3. Radial velocities obtained from the results of observations at the Kourovka Astronomical Observatory 1.2-m telescope. The columns of radial velocities are arranged in the order of spectra 7 to 15 from Table 1

Line	r	V_r, km/s								
		7	8	9	10	11	12	13	14	15
Hβ 4861 Å	0.69	14 ± 5	34 ± 5	-1 ± 6	1 ± 6	23 ± 6	11 ± 6	-72 ± 6	30 ± 5	40 ± 5
Hγ 4341 Å	0.69	9 ± 5	24 ± 5	14 ± 6	0 ± 6	19 ± 6	33 ± 6	-86 ± 6	27 ± 5	41 ± 4
Hα 6563 Å	0.72	8 ± 4	23 ± 4	-1 ± 4	2 ± 4	10 ± 4	6 ± 4	-79 ± 4	26 ± 4	27 ± 4
He I 5876 Å	0.81	25 ± 4	40 ± 4	-20 ± 4	-1 ± 4	28 ± 4	32 ± 4	-61 ± 4	34 ± 4	34 ± 4
He I 4471 Å	0.82	14 ± 5	30 ± 4	6 ± 5	-24 ± 5	27 ± 5	30 ± 5	-77 ± 4	28 ± 4	20 ± 4
He I 6678 Å	0.87	9 ± 6	22 ± 6	6 ± 6			37 ± 6	-68 ± 6	49 ± 5	28 ± 5
He I 4922 Å	0.89	31 ± 7	47 ± 7	-19 ± 7	16 ± 7	29 ± 7	20 ± 6	-27 ± 7	29 ± 7	27 ± 7
He I 5015 Å	0.92	22 ± 7		13 ± 8	10 ± 8	31 ± 8	12 ± 8			
He I 4713 Å	0.93	27 ± 8	29 ± 8	11 ± 9	10 ± 8	21 ± 9		-50 ± 8	60 ± 9	25 ± 8
Mean	–	18 ± 6	31 ± 6	1 ± 6	2 ± 6	24 ± 6	23 ± 6	-65 ± 6	35 ± 6	30 ± 6

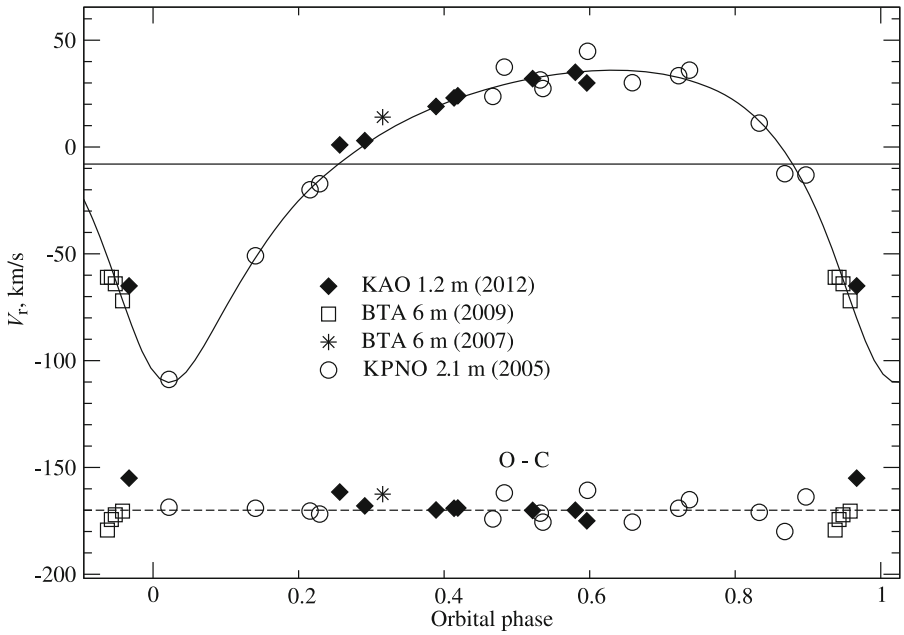

Fig. 3. The velocity curve of HD 37737, constructed from the averaged velocities, given in Tables 2 and 3. The horizontal line at −8 km/s corresponds to the velocity of the system's center of mass. The O−C line is shifted arbitrarily by −170 km/s [2].

eccentricity up to the seventh power of e from [9]:

$$\begin{aligned}\theta = M + \left(2e - 0.25e^3 + \frac{5}{96}e^5 + \frac{107}{4608}e^7\right)\ \sin M \\ + \left(\frac{5}{4}e^2 - \frac{11}{24}e^4 + \frac{17}{192}e^6\right)\ \sin 2M \\ + \left(\frac{13}{12}e^3 - \frac{43}{64}e^5 + \frac{95}{512}e^7\right)\ \sin 3M \\ + \left(\frac{103}{96}e^4 - \frac{451}{480}e^6\right)\ \sin 4M \\ + \left(\frac{1097}{960}e^5 - \frac{5957}{4608}e^7\right)\ \sin 5M \\ + \frac{1223}{960}e^6 \sin 6M + \frac{47273}{32257}e^7\ \sin 7M,\end{aligned} \tag{3}$$

where M is the mean anomaly, which is expressed as:

$$M = \frac{2\pi}{P}(T - T_0). \tag{4}$$

The search for the optimal values of the independent parameters was carried out using a nonlinear least-squares Levenberg–Marquardt method. In addition to the parameters, explicitly present in the equation (2), the value of the system period varied in the approximation process. The initial values of the parameters were taken from [2]. We have initially used the averaged radial velocities, obtained from the list of spectral lines for the search of parameters and construction of the radial velocity curve. The averaging of the velocity values was done separately from the data obtained at each instrument (see Table 2 and 3). As a result of approximation, we were able to refine the value of the orbital period and suggest new ephemerides:

$$\mathrm{JD}_\odot(I_{\min}) = 2453690.23246 + 7\overset{\mathrm{d}}{.}84705\,\mathrm{E}. \tag{5}$$

A new radial velocity curve, constructed using the new ephemerides is shown in Fig. 3.

The presence of the velocity gradient in the stellar atmosphere brings uncertainty in the velocity of the system's center of mass V_{cm}. To estimate this uncertainty we constructed the radial velocity curves of individual lines, and using them we calculated the new parameters of the curves. The results of calculations are presented in Table 4 in the ascension order of the optical depth ($\log \tau_{\mathrm{Ross}}$) of a given spectral line. The specified uncertainties correspond to an error of 1σ. There probably exists a dependence of the velocity of center of mass V_{cm} on the optical depth at which the line is formed. This dependence is controversial, since it is supported by the data of only three lines of helium. A more weaker dependence on the optical depth is probably traced in the half-amplitude values K_1. This may be due to the asymmetry of the atmosphere. A more detailed study will require further observations with high spectral resolution and S/N ratio. As we can see, the estimate of the heliocentric radial velocity

Table 4. Orbital parameters, obtained from the radial velocity curves for different lines are arranged in order of increasing optical depth of the line formation. For the weak lines of He II λ 4686 Å, He I λ 4388 Å, He II λ 4541 Å we used the data only from the 6-m BTA and 2.1-m KPNO telescopes. The listed uncertainties correspond to the error of 1σ. The last line (Mean) contains the parameters determined from the average radial velocity curve (Fig. 3)

Line	$\log\tau_{\rm Ross}$	e	ω, rad	K_1, km/s	$V_{\rm cm}$, km/s	$f(m)$, $M_\odot$	rms, km/s	Number of lines
Hα 6563 Å	−6.75	0.46 ± 0.04	2.85 ± 0.08	60.6 ± 4.5	-11 ± 2	0.13 ± 0.03	5.6	BTA (1), KAO (9)
Hβ 4861 Å	−6.51	0.44 ± 0.02	2.82 ± 0.03	70.4 ± 2.7	-9 ± 2	0.21 ± 0.02	7.8	BTA (5), KAO (9), KPNO (14)
Hγ 4341 Å	−6.29	0.43 ± 0.02	2.80 ± 0.03	75.1 ± 2.6	-11 ± 2	0.25 ± 0.03	7.2	BTA (5), KAO (9), KPNO (14)
He I 5876 Å	−2.39	0.44 ± 0.03	2.74 ± 0.04	74.2 ± 3.2	-8 ± 2	0.24 ± 0.03	8.2	BTA (1), KAO (9)
He I 4471 Å	−1.99	0.43 ± 0.02	2.79 ± 0.03	74.9 ± 3.1	-9 ± 2	0.25 ± 0.03	8.9	BTA (5), KAO (9), KPNO (14)
He I 4922 Å	−1.58	0.44 ± 0.05	2.77 ± 0.06	65.5 ± 5.0	-8 ± 2	0.17 ± 0.04	14.7	BTA (5), KAO (9), KPNO (14)
He II 4686 Å	−1.38	0.43 ± 0.03	2.84 ± 0.05	72.4 ± 4.3	-3 ± 2	0.23 ± 0.04	12.4	BTA (5), KPNO (13)
He I 4388 Å	−1.18	0.44 ± 0.03	2.83 ± 0.04	64.6 ± 5.0	-3 ± 2	0.16 ± 0.04	9.2	BTA (5), KPNO (13)
He II 4541 Å	−0.59	0.43 ± 0.03	2.86 ± 0.04	76.1 ± 3.4	1 ± 2	0.26 ± 0.04	8.5	BTA (5), KPNO (13)
Mean	–	0.44 ± 0.01	2.76 ± 0.02	73.1 ± 1.7	-8 ± 2	0.23 ± 0.02	5.8	BTA (6), KAO (9), KPNO (14)

of the center of mass, calculated from the velocity of individual lines ranges from −11 to 1 km/s.

The last line in Table 4 (Mean) contains the parameters determined from the average radial velocity curve (Fig. 3). One can see that all the values coincide within the measurement errors.

4. PHYSICAL PARAMETERS

4.1. Spectral Type and Luminosity Class

A visual comparison with the spectrum from the spectral atlas by Walborn and Fitzpatrick [10] allows to determine the spectral type of the star as O9.5 III, which is consistent with the previous estimate of Cruz-Gonzalez et al. [11]. In addition, we used the quantitative criteria described in [12, 13] for the O-stars of late spectral types. These criteria are based on the ratios of the equivalent widths of the He I λ 4471 Å and He II λ 4542 Å lines. Measured from the spectra of HD 37737, the value of

$$\log(W_{\lambda\,4471\ \text{Å}}/W_{\lambda\,4542\ \text{Å}}) = 0.52\pm0.04$$

corresponds to the spectral type O9.5.

Determination of the luminosity class is based on the ratio of the equivalent line widths of Si IV λ 4089 Å and He I λ 4143 Å. The measured value of

$$\log(W_{\lambda\,4089\ \text{Å}}/W_{\lambda\,4143\ \text{Å}}) = 0.22\pm0.04$$

corresponds to the luminosity class III. We have additionally measured the value of

$$\log(W_{\lambda\,4388\ \text{Å}}\times W_{\lambda\,4686\ \text{Å}}) = 5.2\pm0.03,$$

which, according to [13], also indicates the luminosity class III. McSwain et al. [2] have obtained the $\log g$ value, which, according to the calibration of [14], corresponds to the luminosity class V, rather than III.

4.2. $T_{\rm eff}$ and $\log g$

In order to solve the above-mentioned discrepancy, the main parameters of the atmosphere of HD 37737 were refined based on the analysis of the BTA spectra, possessing a much higher spectral resolution and S/N ratio than the spectra of [2]. Making the Fourier transform of the observed O II $\lambda\lambda$ 5592, 4185 Å and He I $\lambda\lambda$ 6678, 5876, 5015, 4922, 4471, 4143 Å line profiles, after finding the first zero, the projection of the stellar rotation velocity $v\sin i = 182$ km/s was determined by the method of Carroll, laid out in the monograph of Sakhibullin [15]. The resulting value coincides with that obtained in [2].

The physical parameters of the atmosphere of HD 37737 (effective temperature $T_{\rm eff}$ and the gravitational force on the surface $\log g$) were derived using the OSTAR grid of non-LTE models of stellar atmospheres with solar abundances [16]. The increments of temperature and $\log g$ amounted to 2500 K and 0.25, respectively. The microturbulence velocity was taken to be $V_{\rm mic} = 10$ km/s. An additional study showed that an increase in $V_{\rm mic}$ to 23 km/s does not lead to any noticeable variations in the obtained values of the parameters the atmosphere. The synthetic spectra were calculated using the `SYNSPEC48` code [17]. The convolution with the rotation profile and the instrumental profile in the calculation of this

set of spectra was done using the ROTIN3 code. A combination of model parameters was considered the best, if this combination provided the minimum deviation of the line profiles in the synthetic spectra from the profiles obtained from the observations.

In our analysis we used the lines of hydrogen (Hα, Hβ, Hγ, Hδ) and helium (He I $\lambda\lambda$ 4388, 4471, 4922 Å, He II $\lambda\lambda$ 4200, 4541, 4686, 5411 Å). The deviation was calculated using the formula

$$\chi^2 = \frac{1}{n_{\rm lines}} \sum_{i=0}^{n_{\rm lines}} \frac{w_i}{n_\nu} \sum_{j=1}^{n_\nu} \left(\frac{y_j^i - y_{j\,\rm obs}^i}{\sigma^i} \right)^2, \qquad (6)$$

where n_ν is the number of points on the profile in the spectral line i; $n_{\rm lines}$ is the number of spectral lines which were used in the analysis; $y^i_{j\,\rm obs}$ is the residual intensity in the j-th point of the spectral line i in the spectrum, obtained from observations; y^i_j is residual intensity in the line of synthetic spectrum; w_i is the weight corresponding to the spectral line i; $\sigma^i = (S/N)^{-1}$ accounts for the S/N ratio for the i line. For all the lines the weight was taken to be equal to unity. The studied range of $T_{\rm eff}$ (27 500–35 000 K) and $\log g$ (2.75–4.50) has been selected according to the spectral type of the star.

The above method was applied to the spectra of high spectral resolution, obtained at the 6-m and 1.2-m telescopes. In both cases, the minimum value of χ^2 corresponded to the atmosphere model with $T_{\rm eff} = 30\,000$ K and $\log g = 3.50$. These values, obtained using the methods and observational data, most accurate to date, correspond to the star of spectral type O9.5 III.

4.3. Component Masses

To determine the mass of the star we used the method described by Martins et al. [14]. According to the calibration, the absolute magnitude for stars of spectral type O9.5 III is $M_V = -5.174$. The bolometric correction for a star with an effective temperature of $T_{\rm eff} = 30\,000$ K amounts to BC $= -2.864$, respectively. The resulting value of the absolute magnitude corresponds to the radius of the star $R = 13.4 \pm 0.9\ R_\odot$. Next, using the relation between the fundamental parameters of the star and the parameters of the atmosphere, from the values of $T_{\rm eff} = 30\,000$ K and $\log g = 3.50$ we get the mass estimate of the primary component of HD 37737, which is $M_1 = 26 \pm 2\ M_\odot$. The resulting mass of the primary component in combination with the mass function is $f(m) = 0.23 \pm 0.02\ M_\odot$ (see Table 4) allows us to estimate the mass of the secondary component of the binary, $M_2 > 6.2 \pm 0.5\ M_\odot$. Thus, the primary component of the HD 37737 binary system is a massive star and the secondary is an intermediate-mass or a massive star.

ACKNOWLEDGMENTS

The authors thank E. L. Chentsov and S. Yu Parfyonov for the assistance. This work was supported in part by the federal target program Research and Development in Priority Areas of Science and Technology of Russia 2007–2013 (state contract no. 14.518.11.7064). M. V. Yushkin thanks the Russian Foundation for Basic Research for the partial financial support of this study (grant no. 12-07-00739). The observations at the 6-m telescope are supported by the Russian Ministry of Education and Science (state contracts no. 14.518.11.7070 and 16.518.11.7073).

REFERENCES

1. D. R. Gies and C. T. Bolton, Astrophys. J. Suppl. **61**, 419 (1986).
2. V. McSwain, T. S. Boyajian, E. D. Grundstrom, et al., Astrophys. J. **655**, 473 (2007).
3. E. L. Chentsov and A. N. Sarkisyan, Astrophysical Bulletin **62**, 257 (2007).
4. S. Yu. Gorda, P. E. Zakharova, V. V. Krushinsky, E. D. Kuznetsov in *Proc. of 38th International Student Conference Physics of Space* (USU Publishing, Ekaterinburg, 2009), p. 110.
5. V.E. Panchuk, M. V. Yushkin, and M. V. Yakopov, Astrophysical Bulletin **66**, 355 (2011).
6. G. A. Galazutdinov , SAO Preprint No. 92 (SAO RAS, Nizhnii Arkhyz, 1992).
7. V. E. Panchuk, V. G. Klochkova, M. V. Yushkin, and I. D. Naidenov, J. Opt. Tech. **76**, 87 (2009).
8. M. J. Kurtz, D. J. Mink, W. F. Wyatt, et al., ASP Conf. Ser. **25**, 432 (1992).
9. D. Brauer, J. Clemens, *Metodi nebesnoi mehaniki (Methods of Celestial Mechanics)* (Mir, Moscow, 1964) [in Russian].
10. N. R. Walborn and E. L. Fitzpatrick, PASP **102**, 379 (1990).
11. C. Cruz-Gonzalez, E. Recillas-Cruz, R. Costero, et al., Revista Mexicana de Astronomia y Astrofisica **1**, 211 (1974).
12. P. S. Conti and W. R. Alschuler, Astrophys. J. **170**, 325 (1971).
13. G. Mathys, Astronom. and Astrophys. Suppl. **76**, 427 (1988).
14. F. Martins, D. Schaerer, and D. J. Hillier, Astronom. and Astrophys. **436**, 1049 (2005).
15. N. A. Sakhibullin, *Metodi modelirovaniya v astrofizike (Modeling Methods in Astrophysics)*, Vol. 2 (Fen, Kazan, 2003) [in Russian].
16. T. Lanz and I. Hubeny, Astrophys. J. Suppl. **147**, 225 (2003).
17. I. Hubeny and T. Lanz, Astrophys. J. Suppl. **262**, 501 (1992).